

https://doi.org/10.1070/QEL17559

Quantum transport in a one-dimensional flux rhombic lattice

P.S. Muraev, A.R. Kolovsky

Abstract. **We analyse stationary current of the bosonic particles in a flux rhombic lattice connecting two particle reservoirs. For vanishing interparticle interactions the current is shown to monotonically decrease as the flux is increased and become strictly zero for the Peierls phase equal to π. Nonzero interactions modify this dependence and for moderate interaction strength the current is found to be independent of the flux value.**

Keywords: *quantum transport, rhombic lattice, pseudoclassical approach.*

1. Introduction

Quantum transport through periodic structures has been of permanent interest since the early days of quantum mechanics [1]. Recently this problem has been addressed for cold atoms in optical lattices where one of the research directions is the transport of Bose or Fermi atoms between two reservoirs which are connected by a lattice [2–9]. Remarkably, under certain conditions this problem can be solved analytically, which will become a reference point for studying different realistic systems. Roughly, these conditions are the following: (i) the reservoirs are Markovian so that one can justify a master equation for the reduced density matrix for the fermionic/bosonic carriers in the lattice; (ii) interparticle interactions are negligible so that we can use the formalism of the single-particle density matrix; and (iii) the lattice has a simple structure and can be approximated by the linear tight-binding chain. Violation of any of these conditions makes the system much harder for analysis but, simultaneously, introduces new effects. In particular, it has been recently shown [9] that interparticle interactions change the ballistic transport regime, where the current is independent of the lattice length, into the diffusive transport regime, where the current is inversely proportional to the lattice length.

In the present work we extend the studies of Ref. [9] by considering the transport of Bose particles through the rhombic lattice. The Bloch spectrum of this lattice is known to consist of two dispersive bands and one flat band which is formed by the localised states. Moreover, by applying an external gauge field one can modify the dispersion relation of the dispersive bands, making them flat as well [10–12]. These relate the problem considered in the paper to the other fundamental problems like the role of flat bands in the quantum transport [13–15] and the stability of the localised states in the presence of interparticle interactions [10, 16, 17].

The cold-atom realisation of a quasi one-dimensional optical lattice, which is close to a flux rhombic lattice, was reported in Ref. [18], where squares (the so-called two-leg ladder) were used instead of rhombs. Varying the flux of the synthetic magnetic field through the square, Atala et al. [18] convincingly demonstrated the change in the Bloch dispersion relation but the case of flat bands, unfortunately, cannot be reached with the square geometry. We also mention that the flux rhombic lattice can be viewed as a chain of identical Mach–Zehnder interferometers with different arm lengths. This analogy might suggest a very different physical realisation of the model. However, to be certain, we shall keep in mind the cold-atom realisation where the Bose atoms are loaded into the optical lattice of the considered specific geometry.

2. System

The elementary cell of the rhombic lattice consists of three sites which we denote by letters C_m, A_m, and B_m, where the subscript m denotes the cell number (Fig. 1). We assume the presence of the magnetic flux through each cell characterised by the Peierls phase Φ. Then the Bloch bands are given by the equation

$$\varepsilon_0(\kappa) = 0, \quad \varepsilon_\pm(\kappa) = \pm J\sqrt{1+\cos(\Phi/2)\cos(\kappa-\Phi/2)}, \qquad (1)$$

where κ is the quasi-momentum, and $\varepsilon_0(\kappa)$ is the flat band energy. Of a particular interest is the case $\Phi = \pi$, where the dispersive bands $\varepsilon_\pm(\kappa)$ become flat, that is $\varepsilon_\pm(\kappa) = \pm J$.

The system Hamiltonian is of the Bose–Hubbard type,

$$H = -\frac{1}{2}\sum_{l,m}(J_{lm}\hat{a}_m^\dagger\hat{a}_l + \text{h.c.}) + \frac{U}{2}\sum_l \hat{n}_l(\hat{n}_l - 1), \qquad (2)$$

where $|J_{lm}| = J$ is the atomic hopping rate between the lattice sites, the parameter U characterises the strength of the collision-like interatomic interactions, and $\hat{n}_l$ is the operator of the number of particles. We chose to work with the gauge where the matrix element $J_{CA} = J\exp(i\Phi/2)$, the matrix element $J_{CB} = J\exp(-i\Phi/2)$, and the remaining two matrix elements equal J. For the numerical purpose we

P.S. Muraev, A.R. Kolovsky Kirensky Institute of Physics, Siberian Branch, Russian Academy of Sciences, Akademgorodok 50, stroenie 38, 660036 Krasnoyarsk, Russia; Siberian Federal University, prosp. Svobodnyi 79, 660041 Krasnoyarsk, Russia; e-mail: muraev.pavel@mail.ru

Received 16 March 2021
Kvantovaya Elektronika **51** (6) 502–505 (2021)
Submitted in English

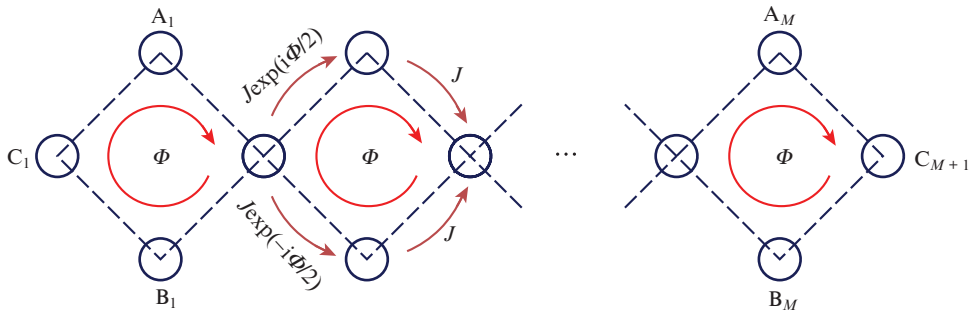

Figure 1. Flux rhombic lattice consisting of M rhombs. The flux is characterised by the Peierls phase Φ which determines the values of the hopping matrix elements.

reorder the lattice sites as C_1, A_1, B_1, C_2, A_2, B_2, ... (thus, for example, the subscript $l = 5$ corresponds to the A site in the second cell).

We are interested in the transport of Bose particles across the rhombic lattices where particles come from the left reservoir into the site C_1 and go out of the lattice into the right reservoir from the site C_{M+1}. The presence of particle reservoirs converts the Hamiltonian system (2) into the open many-body system whose dynamics is described by the reduced density matrix $R(t)$ of the carriers in the lattice. In the simplest case, which implies the validity of the Born–Markov approximation [19], the master equation for the reduced density matrix R has the form [6–9]

$$\frac{\mathrm{d}R}{\mathrm{d}t} = -\mathrm{i}[H, R] + L_{\mathrm{source}}(R) + L_{\mathrm{drain}}(R), \tag{3}$$

where the operator

$$L_{\mathrm{source}}(R) = -\frac{\gamma_{\mathrm{L}}}{2}[(\bar{n}_{\mathrm{L}} + 1)(\hat{a}_1^{\dagger}\hat{a}_1 R - 2\hat{a}_1 R\hat{a}_1^{\dagger} + R\hat{a}_1^{\dagger}\hat{a}_1)$$

$$+ \bar{n}_{\mathrm{L}}(\hat{a}_1\hat{a}_1^{\dagger}R - 2\hat{a}_1^{\dagger}R\hat{a}_1 + R\hat{a}_1\hat{a}_1^{\dagger})] \tag{4}$$

and the operator

$$L_{\mathrm{drain}}(R) = -\frac{\gamma_{\mathrm{R}}}{2}[(\bar{n}_{\mathrm{R}} + 1)(\hat{a}_L^{\dagger}\hat{a}_L R - 2\hat{a}_L R\hat{a}_L^{\dagger} + R\hat{a}_L^{\dagger}\hat{a}_L)$$

$$+ \bar{n}_{\mathrm{R}}(\hat{a}_L\hat{a}_L^{\dagger}R - 2\hat{a}_L^{\dagger}R\hat{a}_L + R\hat{a}_L\hat{a}_L^{\dagger})] \tag{5}$$

take into account the processes of particle exchange between the system (the lattice) and reservoirs. The parameters γ_{L} and γ_{R} and the parameters $\bar{n}_{\mathrm{L}}$ and $\bar{n}_{\mathrm{R}}$ in Eqns (4) and (5) are the exchange rates and particle density of the left and right reservoirs, respectively. Note that the usage of the terms 'source' and 'drain' in Eqns (3)–(5) implies that $\bar{n}_{\mathrm{L}} > \bar{n}_{\mathrm{R}}$.

In the subsequent sections we solve Eqn (3) and calculate the single-particle density matrix (SPDM) of the carriers,

$$\rho_{lm}(t) = \mathrm{Tr}[\hat{a}_l^{\dagger}\hat{a}_m R(t)], \quad 1 \leqslant l, m \leqslant L, \tag{6}$$

which suffices to predict the particle current between the reservoirs. The size of this matrix is obviously given by $L = 3M + 1$, where M is the number of rhombs.

3. Noninteracting particles ($U = 0$)

In the case of vanishing interparticle interactions one can obtain a closed set of ordinary differential equations for the SPDM elements,

$$\frac{\mathrm{d}}{\mathrm{d}t}\rho_{lm}(t) = -\mathrm{i}[H, \hat{\rho}]_{lm} - \sum_{j=1,L}\frac{\gamma_j}{2}(\delta_{lj} + \delta_{mj})\rho_{lm}$$

$$+ \sum_{j=1,L}\gamma_j\bar{n}_j\delta_{lj}\delta_{mj}. \tag{7}$$

Note that this equation is valid for any lattice as soon as the particles are injected in the first site of the lattice and withdrawn from the last site. In what follows, to simplify equations, we assume that the relaxation constants $\gamma_1 \equiv \gamma_{\mathrm{L}}$ and $\gamma_L \equiv \gamma_{\mathrm{R}}$ are the same and equal to γ.

Let us first discuss the case $\Phi = 0$ where Eqn (7) can be solved analytically. The stationary SPDM of the bosonic carriers in the rhombic lattice is exemplified in the lower-left corner in Fig. 2 for $M = 7$. Here the stationary populations of the C sites are the same (except the first and last sites) and are given by the equation,

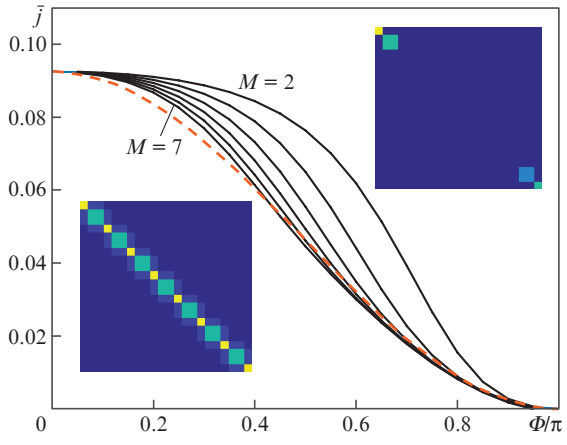

Figure 2. (Colour online) Normalised stationary current as a function of Φ for $M = 2$–7. The following parameters are used: $\gamma_{\mathrm{L}} = \gamma_{\mathrm{R}} = 0.4J$ and $\bar{n}_{\mathrm{R}}/\bar{n}_{\mathrm{L}} = 0.5$. The dashed line corresponds to Eqn (12). The inserts show the elements of the stationary SPDM by the absolute values for $M = 7$ and $\Phi = 0$ (lower-left corner) and π (upper-right corner).

$$\rho_{ll}^{\mathrm{C}} = \frac{\bar{n}_{\mathrm{L}} + \bar{n}_{\mathrm{R}}}{2}, \tag{8}$$

and populations of the A and B sites are one half of this value. Furthermore, the off-diagonal elements ρ_{lm} (here l and m are the nearest two lattice sites) are the same. These elements determine the mean current of the Bose atoms across the lattice, which obeys the equation

$$\bar{j} = j_0 \frac{J\gamma}{J^2 + \gamma^2/2} \frac{\bar{n}_{\mathrm{L}} - \bar{n}_{\mathrm{R}}}{2}, \tag{9}$$

where $j_0 = Jd/\hbar$ and d is the lattice period. Comparing this equation with Eqn (34) in Ref. [9] we conclude that for $\Phi = 0$ the rhombic lattice behaves similar to the simple linear lattice with the even sites given by the 'sum' of the A and B sites of the rhombic lattice. We also mention that the difference $\bar{n}_{\mathrm{L}} - \bar{n}_{\mathrm{R}}$ can be rewritten as $\bar{n}_{\mathrm{L}}(1 - \bar{n}_{\mathrm{R}}/\bar{n}_{\mathrm{L}})$. Then, by normalising the stationary current $\bar{j}$ by $j_0\bar{n}_{\mathrm{L}}$, it becomes the function of only two parameters, that is, the ratio $\bar{n}_{\mathrm{R}}/\bar{n}_{\mathrm{L}}$ and the ratio γ/J.

Next we analyse the case $\Phi = \pi$ (see the upper-right corner in Fig. 2). As expected, here the propagation of particles across the lattice is blocked by the destructive interference and the current is strictly zero. For populations of the edge sites we have

$$\rho_{ll} = \bar{n}_{\mathrm{L}}, \quad \rho_{LL} = \bar{n}_{\mathrm{R}}, \tag{10}$$

and populations of the neighbouring A and B sites are one half of these values. Note also that the A–B dimers at the lattice edges are in the antisymmetric (left edge) and the symmetric (right edge) states, that is,

$$\rho_{\mathrm{AB}} = \mp\sqrt{\rho_{\mathrm{AA}}\rho_{\mathrm{BB}}}\,. \tag{11}$$

Unfortunately, there is no simple analytical expression for the stationary current for an arbitrary Φ. Moreover, the result depends on the lattice length. The main panel in Fig. 2 shows the stationary current in the system as the function of Φ for $2 \leqslant M \leqslant 7$ (the current is normalised to the particle density in the left reservoir). It is seen that the curves rapidly converge to some limiting curve which can be approximated by the relation

$$\bar{j}(\Phi) \approx \bar{j}(\Phi = 0)\cos^2(\Phi/2). \tag{12}$$

One may naively assume that dependence (12) is given by the mean squared group velocity of a quantum particle in the lattice [8]; however, this appears to be not the case. A proof of Eqn (12) remains an open problem.

4. Interacting particles

To treat the case of interacting particles we use the pseudo-classical approach (also known as the truncated Wigner function or truncated Husimi function approximations), which was proved to be very accurate when analysing the current in the simple linear lattice [9]. This approach reduces the master equation (3) to the Fokker–Planck equation on the classical distribution function $f = f(\boldsymbol{a}, \boldsymbol{a}^*; t)$ defined in the multi-dimensional phase space $\boldsymbol{a} = a_1, \ldots, a_L$:

$$\frac{\partial f}{\partial t} = \{H, f\} + \sum_{l=1,L} [G^{(l)}(f) + D^{(l)}(f)], \tag{13}$$

where H is the classical counterpart of the Bose–Hubbard Hamiltonian (2), $\{\ldots,\ldots\}$ denotes the Poisson brackets, and the terms in the square brackets are the Weyl images of the Lindblad operators $L_{\mathrm{source}}(R)$ and $L_{\mathrm{drain}}(R)$. To clarify the mathematical structure of the equation, we explicitly decompose these images into the friction terms,

$$G^{(l)}(f) = \frac{\gamma_l}{2}\left(a_l \frac{\partial f}{\partial a_l} + 2f + a_l^* + \frac{\partial f}{\partial a_l^*}\right), \tag{14}$$

and the diffusion terms

$$D^{(l)}(f) = D_l \frac{\partial^2 f}{\partial a_l \partial a_l^*}, \tag{15}$$

where the diffusion coefficients $D_1 \equiv D_{\mathrm{L}}$ and $D_L \equiv D_{\mathrm{R}}$ are proportional to the reservoir particle densities $\bar{n}_{\mathrm{L}}$ and $\bar{n}_{\mathrm{R}}$, respectively.

Knowing the distribution function $f = f(\boldsymbol{a}, \boldsymbol{a}^*; t)$, the SPDM elements are calculated by taking the multi-dimensional integral

$$\rho_{lm}(t) = \int a_l^* a_m f(\boldsymbol{a}, \boldsymbol{a}^*; t)\, \mathrm{d}\boldsymbol{a}\mathrm{d}\boldsymbol{a}^*. \tag{16}$$

Note that the method is exact for $U = 0$ and in the formal limit $U \to 0$, $\bar{n}_{\mathrm{L}} \to \infty$, $g = U\bar{n}_{\mathrm{L}} = \mathrm{const}$. The main advantage of the approach is that, when we cannot solve Fokker–Planck equation (13) analytically, it is always possible to estimate $\rho_{lm}(t)$ by mapping this equation into the Langeven equation and then employing the Monte-Carlo simulation.

Figure 3 compares the stationary current in the flux rhombic lattice as $g = 0$, 0.7, and 2. It is seen that for Φ close to zero, interactions suppress the current. This is consistent with the results of Ref. [9] and, in fact, is an indication of the transition from the ballistic transport regime to the diffusive regime. For Φ close to π, however, the current is enhanced and has a finite value even for $\Phi = \pi$ where transport is for-

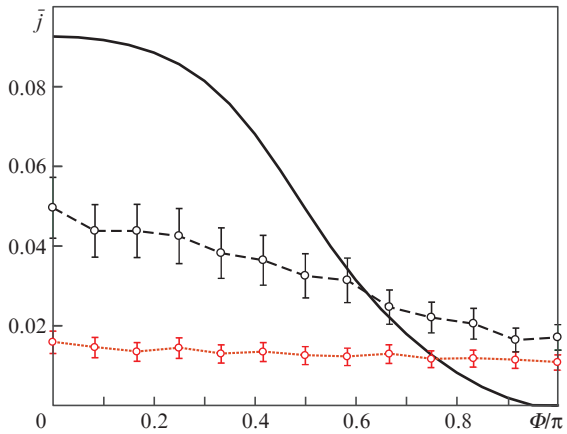

Figure 3. Stationary current as a function of Φ for $M = 5$ and $g =$ (solid line) 0, (dashed line) 0.7, and (dash-dotted line) 2. The other parameters are the same as in Fig. 2. The error bar indicates statistical error due to the Monte-Carlo simulation.

bidden due to the localisation effect if $g = 0$. Thus, interactions destroy the localisation. This is consistent with results of Ref. [10], which analyses the energy spectrum of two interacting fermions in the flux rhombic lattice, and results of Ref. 17], which specifically addresses the stability of the localised states against interactions. In particular, it was shown in the latter work that the antisymmetric (or symmetric, depending on the chosen gauge) localised A – B state is subject to dynamical instability which leads to excitation of the unprotected symmetric (antisymmetric) A – B state. Because the developing of instability takes some time, in the rhombic lattice we have very long transient regime for $\Phi = \pi$. During this transient process we observe subsequent populations of the C sites with the time delay given by the instability time (Fig. 4). When all C sites are populated, the system reaches the steady-state regime with the diffusive-like transport from the left to the right reservoirs.

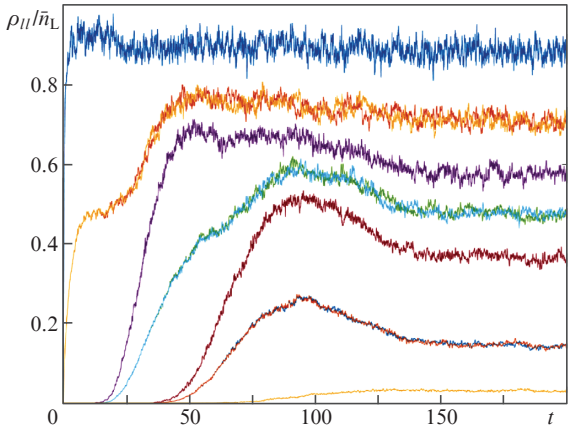

Figure 4. (Colour online) Population of the lattice sites (diagonal elements of the SPDM) as a function of time for $\Phi = \pi$ and $M = 3$. The other parameters are $\gamma_L = \gamma_R = 0.4J$, $\bar{n}_R = 0$, and $g = 4$. Averaging is performed over 400 realisations. Different curves refer to $\rho^{(1)}_{CC}, \rho^{(1)}_{AA}$ and $\rho^{(1)}_{BB}, \rho^{(2)}_{CC}, \rho^{(2)}_{AA}, \rho^{(2)}_{BB}$, etc., from top to bottom. The time t is normalised to the tunnelling time h/J.

The used pseudo-classical approach also provides an alternative viewpoint on the role of interparticle interactions for the quantum transport. While in the quantum picture the account for interactions leads to degradation of coherent properties of the SPDM, in the classical picture, where interacting bosons in each lattice site are viewed as classical nonlinear oscillators, the loss of coherence is related to the dephasing (de-synchronisation) between different oscillators due to the fact that the frequency of a nonlinear oscillator depends on its amplitude.

5. Conclusions

We studied the current of noninteracting and interacting bosonic carriers across the flux rhombic lattice. In the case of vanishing interparticle interactions the transport is ballistic and the current is determined by the interference effects due to the presence of two alternative passes between the C sites. For the zero flux the interference is constructive and the current is maximal. On the contrary, for the flux corresponding to the Peierls phase $\Phi = \pi$, the interference is completely destructive and the current is zero. For the intermediate value of Φ, the current was found to be approximately proportional to $\cos^2(\Phi/2)$.

Unlike the case of vanishing interactions, for a moderate interaction strength $g \approx J$ the current is mainly determined by the interaction effects, which change the ballistic transport regime into diffusive transport. It can be expected from general arguments that diffusion destroys interference. This expectation was fully confirmed by the straightforward numerical analysis of the system dynamics where the stationary current of the bosonic carries was found to be essentially independent of the flux.

Acknowledgements. This work was supported by the Russian Science Foundation (Grant No. 19-12-00167).

References

1. Bloch F. *Z. Phys*., **52**, 555 (1928).
2. Lebrat M., Grisins P., Husmann D., Häusler S., Corman L., Giamarchi T., Brantut J.-Ph., Esslinger T. *Phys. Rev. X*, **8**, 011053 (2018).
3. Prosen T., Žunkovič B. *New J. Phys*., **12**, 025016 (2010).
4. Znidaric M. *J. Stat. Mech*., **2010**, L05002 (2010).
5. Bruderer M., Belzig W. *Phys. Rev. A*, **85**, 013623 (2012).
6. Ivanov A., Kordas G., Komnik A., Wimberger S. *Eur. Phys. J. B*, **86**, 345 (2013).
7. Kordas G., Witthaut D., Wimberger S. *Ann. Phys*., **527**, 619 (2015).
8. Kolovsky A.R., Denis Z., Wimberger S. *Phys. Rev. A*, **98**, 043623 (2018).
9. Bychek A.A., Muraev P.S., Maksimov D.N., Kolovsky A.R. *Phys. Rev. E*, **101**, 012208 (2020).
10. Vidal J., Doucot B., Mosseri R., Butaud P. *Phys. Rev. Lett*., **85**, 3906 (2000).
11. Longhi S. *Opt. Lett*., **38**, 3570 (2013).
12. Mukherjee S., Thomson R.R. *Opt. Lett*., **40**, 5443 (2015).
13. Khomeriki R., Flach S. *Phys. Rev. Lett*., **116**, 245301 (2016).
14. Kolovsky A.R., Ramachandran A., Flach S. *Phys. Rev. B*, **97**, 045120 (2018).
15. Kun Woo Kim, Andreanov A., Flach S. *Phys. Rev. Res*., **2**, 023067 (2020).
16. Danieli C., Andreanov A., Flach S. *Phys. Rev. B*, **102**, 041116 (2020).
17. Maksimov D.N., Bychek A.A., Kolovsky A.R. *Phys. Rev. A*, **102**, 033324 (2020).
18. Atala M., Aidelsburger M., Lohse M., Barreiro J.T., Paredes B., Bloch I. *Nat. Phys*., **10**, 588 (2014).
19. Kolovsky A.R. *Phys. Rev. E*, **101**, 062116 (2020).